

Fuzzy-Controlled Living Insect Legged Actuator

Chao Zhang, Feng Cao, Yao Li, Hirotaka Sato*

School of Mechanical and Aerospace Engineering,
Nanyang Technological University, 639798, Singapore

*Corresponding Author. Tel: +65 6790 5010
E-mail address: hirosato@ntu.edu.sg

ABSTRACT

Steering motor units (e.g. legs) of a living organism by controlled stimulation protocols is a key performance toward living machines, biohybrid robots, or cyborg animals — a fusion of living organisms and man-made devices. To achieve fundamental locomotion pattern generation (e.g. walking gait), a closed-loop (feedback) control system to steer motor units to be set at or to move along a predetermined position and motion path is essential. This study demonstrated the capability to build a precise closed-loop control system manipulating the angular displacement of a coleopteran's leg with electrical stimulation applied directly to the corresponding muscles. We confirmed the correspondence between the angular displacement of the beetle's leg and the electrical stimulation frequency was proportional, nonlinear, and time-variant. A fuzzy control system with multiple membership functions using a proportional controller with adjustable parameters was then proposed and adopted for motion control, and we successfully steered a living leg along a predetermined motion path.

Keywords: Fuzzy Control, Biohybrid Robots, Insect Motion Control, Insect Muscle Control

1 **1. Introduction**

2 Inspirations from nature are essential for breakthroughs in robot design. Besides complicated
3 robotic networks with artificial intelligence functions, the emerging production of living
4 machines, biohybrid robots, or cyborg animals [1] targets the combination of merits from both
5 man-made devices and biological organisms, which makes this research field a highly
6 discussed topic of great practical interest. A living machine involves imitation or direct
7 utilization of functional biological elements, from molecules, such as enzymes, cells to tissues,
8 or even to an entire organism, incorporated into artificial context with the desired real-time
9 control [1-3].

10 What are the merits of using biological organisms for living machines compared with
11 entirely man-made ones? Living organisms, especially insects, possess many excellent
12 properties, including outstanding and unparalleled agility of locomotion, which has made
13 insects among the top focuses in the development of autonomous robots for decades [4-19].
14 Employing living insects as the platform for legged machines by electrical stimulation on leg
15 muscles to induce user desired motor actions and behaviors leads to significant power-saving.
16 The electrical stimulation of muscle tissues consumes power on the order of a few hundred
17 microwatts, whereas the power consumption of man-made legged robots with mechatronics
18 components is on the order of 100–1000 mW [7, 20, 21]. Complicated control algorithms,
19 accurate motors, and sensing devices developed with knowledge from bionics are essential for
20 man-made robots to retain their postures and to traverse obstacles. On the contrary, majority
21 of such complicated control algorithms and devices are not necessary for living legged-
22 machines made of insects' muscle tissues. The user is able to utilize the insect's intrinsic
23 walking system. For example, when the living-legged machine comes across an obstacle, the
24 user shuts off the stimulator and releases the living insect platform from the user's command
25 and control system to let the insect overcome or avoid the obstacle by itself.

26 Toward living legged 'machine' or 'robot' (walking control), as a starter, we attempt to
27 have legged 'actuator' (one leg motion control). Fine control of one leg motion would finally
28 lead to machine or robot. We have successfully performed control of walking gaits by
29 stimulating insect leg muscles and regulating two legs' motions under predetermined
30 sequence [22]. To regulate leg motion precisely and navigate the machine under control, the
31 motions of each leg and machine itself should be monitored. In laboratory environment, this
32 study used a [vision](#)-based feedback where a motion capture system consisting of external
33 cameras is employed to have 3D positional information of the legs. For open environment
34 outside laboratory, it would be possible in future to use MEMS (micro electro mechanical
35 systems) gyroscopes and acceleration meters, which should be attached on insect legs, to
36 obtain feedback information on both angular and linear motions for a closed-loop control.
37 [Micro navigation systems for miniature aerial vehicles have been widely deployed \[23-28\].](#)
38 [Chowdhary et al. integrate off-the-shelf low cost range sensors into a navigation system](#)
39 [functional in GPS denied indoor environments \[24\].](#) [Brown et al. developed a miniature, low](#)
40 [cost integrated GPS/inertial system designed to navigate unmanned aerial vehicle in a small](#)
41 [self-contained package < 1 cubic inch including a triad of accelerometers and gyroscopes \[23\].](#)
42 [Some researchers have attempted to develop tiny electronic nodes which wirelessly](#)
43 [communicate with one another or a remote console \[29-34\] Such a node has self-powering](#)
44 [unit \(energy scavenger, energy harvester\), for which some piezo acoustic power generators,](#)
45 [solar cells and biofuel cells has been proposed, designed and demonstrated. Such a self-](#)
46 [powered node can be integrated with MEMS gyroscope, accelerometer and electrical](#)
47 [stimulator. Assuming a practically usable self-powered node would be available in future, we](#)
48 [would be able to implant or insert such nodes into muscles of interest and make them](#)

49 communicate with the remote console at user (probably via a microcomputer mounted on the
50 insect back considering the transmitter of the node should be very low). Such integrated
51 wireless node has not been practically demonstrated yet but the self-powering unit and micro
52 sensors have been designed, manufactured and demonstrated. Once such an integrated
53 wireless node is practically available, we can eliminate wiring electrodes into muscles in
54 insect legged actuators and robots.

55 The practical use of living machines that directly involves functional biological elements
56 entails three major challenges: (1) using a large biological unit (e.g. living muscle), (2)
57 keeping the biological unit in its functional environmental conditions (e.g. saline medium),
58 and (3) advancing from open-loop control demonstration to the adaptation of a closed-loop
59 (feedback) control system to steer the biological element (e.g. insect leg) to follow a
60 predetermined motion path. As for (1) and (2), a few demonstrations have been conducted for
61 living-muscle-based machines, while various biosensors using small biological units, such as
62 enzymes, antibodies, and living cells, have been developed to date. Akiyama et al.
63 demonstrated the possibility of building motor units by using muscle tissues extracted from
64 living insects and kept in a specially designed chemical solution environment [2, 35, 36].
65 They demonstrated the chemical stimulation of the insect's muscle tissues. To avoid the
66 maintenance of the working environment, the researchers including the authors did not extract
67 insect muscles but directly used an intact insect leg for building a biological actuator for
68 toward-living-legged machines [20]. Electrical stimulation of large muscle tissues in a living
69 body not only demonstrated the possibility incorporating large biological units of living
70 muscles but also maintained its functional environmental conditions (muscular physiology
71 was self-maintained by the insect as the muscle was not extracted but kept inside the cuticles)
72 for long-term utilization with low power consumption [20, 37]. Furthermore, the researchers
73 also demonstrated a conventional control system with a single proportional controller on
74 muscle motion to steer the leg to follow a user-predetermined motion path [20].

75 Many researchers have targeted varieties of insect neuromuscular sites for stimulation,
76 including brain, ganglia, nerve cords, sensory units (e.g. antenna, compound eyes), and
77 muscles for achieving locomotion control or appendage motion [4-7, 9-11, 38-44]. Most of
78 the stimulation protocols proposed and tested were conducted in open-loop control manner
79 [4-7, 9-11]. Those researches focused on developing effective stimulation protocols, e.g. to
80 find "What stimulation applied to which neuromuscular sites can elicit desired motor actions
81 and behaviors at how much success rate?". A fundamental issue in the stimulation protocols,
82 where stimulated targets were neural sites other than muscle, was that the stimulation does not
83 guarantee 100% success rate in inducing desired motion. On the other hand, the muscle
84 stimulation demonstrated in the authors' previous research [20, 22] resulted in 100% success
85 rate in inducing desired leg motions (for example, if the levation muscle is stimulate, no other
86 motion but only the levation motion is induced), in which specific leg muscle groups were
87 individually and separately stimulated via the properly implanted electrodes. Based on such a
88 reliable electrical stimulation targeting leg muscle groups, they demonstrated the
89 abovementioned conventional control system. Despite the successful demonstration,
90 considerably large overshoot, long response time, and severe fluctuation were observed [20].
91 Hence, for a more sophisticated and precise motion control, it is important to determine the
92 inherent characteristics of an actuator based on biological material (e.g. insect leg muscle),
93 and then to investigate possible solutions.

94 Functional electrical stimulation (FES), which intentionally induces and regulates
95 desired motor action in limb of polarized patient (or experimental mammals as starter), has
96 been intensively researched. Electrically induced rotation of the limb around the joint can be

97 mathematically modelled and controlled by modulating the intensity of stimulation delivered
98 to, for example, the flexor and extensor muscles [45-51]. FES researchers have successfully
99 developed many sophisticated open-loop, rule-based, or feedback controlled FES systems
100 capable of rejecting instantaneous disturbances. Muscle response to electrical stimulation is
101 nonlinear and time-varying, and is also subject to unpredictable reflexes that may generate
102 perturbations [46, 50-52]. Muscle fatigue is also a significant factor in the time-varying nature
103 of the stimulated muscle response [53]. Due to such characteristics, conventional
104 proportional-integral-derivative (PID) controllers adopted for regulating limb rotation have
105 large overshoot, slow rise and settling time, and are sensitive to model mismatch errors [49].
106 Researchers have then developed fuzzy controls for better performance in regulating limb
107 rotation. Fuzzy control, such as the gain scheduling controller, yielded a slow response with
108 little overshoot [45, 49, 50]. [Even though the target animal in this paper is not human nor any
109 other vertebrate but insect, the outcomes from human and vertebrate researches help to
110 develop similar strategies for the insect motion control.](#)

111 We confirmed a major characteristic of biological material is that, unlike a traditional
112 man-made mechatronics system, the response of biomaterial based on insects (e.g. insect leg
113 muscle) to electrical stimulation can neither be mathematically modeled in practice nor
114 uniquely defined in details [38-44]. There is a clear tendency that the motion response of leg
115 muscles is monotonically increased by the frequency of electrical stimulation with fixed
116 stimulation period to its maximum angular displacement position corresponding to an
117 maximum stimulation frequency ceiling [6, 20, 38-41, 54]. However, an undefined hysteresis
118 property also clearly exists in the leg response, which is demonstrated in details in this paper.
119 Our research in this paper concludes that biomaterial of insect muscle tissues is a nonlinear
120 and time-variant system with hysteresis property. There is a clear difficulty in designing a
121 refined conventional control system based on PID controller for such nonlinear time-variant
122 system in practice. The analytical optimization of the parameters for the conventional PID
123 controller and the stability and robustness of such control system are not guaranteed.

124 To address the abovementioned problematic characteristic, in this study, we propose to
125 adopt a fuzzy logic for a refined precision feedback control on a biological actuator (e.g.
126 insect's leg motion control). A fuzzy-logic-based control system analyzing analog input
127 values defined in an ambiguous status works better with nonlinear and time-variant systems
128 compared with conventional PID controller [55-58]. Characteristics of the beetle leg muscle
129 as biological materials, such as hysteresis property, make the input values, namely the
130 feedback on angular displacement, defined in an ambiguous relative status in terms of its
131 corresponding stimulation frequency. Clearly, a higher stimulation frequency leads to a larger
132 angular displacement of the beetle's leg motion [20]. However, the standard for a higher
133 stimulation frequency or a larger angular displacement was relatively, rather than absolutely,
134 defined. A fuzzy control system can adjust its internal parameters according to different
135 situations through membership functions.

136 Another benefit from the fuzzy control system is its simplicity and minimum power
137 requirement for hardware, which is significant as we aim to develop a reliable miniature
138 legged robot with live beetle carrying mechatronic controller on its back. The fuzzy control
139 method does not require convergence of the system. Thus the same design fuzzy control
140 method can be applied on different beetles which do not have exactly the same response to
141 the same electrical stimulation. And the parameters of the fuzzy control method can be
142 quickly calibrated in practice due to its structural simplicity to achieve its optimal
143 performance.

144 In this study, we adopted a fuzzy control system for precision motion control of an insect
145 leg. The individual membership function for fuzzification, namely adjustment of internal
146 parameters of a proportional controller, was applied to every single feedback. The fuzzy
147 control system achieved better performance, i.e. smaller overshoot, shorter reaching time (the
148 time between the change in desired input angle and the first reach of the desired angle of the
149 beetle's leg), and less fluctuation, compared with that achieved by a conventional control
150 system using a single proportional controller.

151 152 153 **2. Materials and Methods**

154 *2.1. Insect for study and electrical stimulation device*

155 *Mecynorrhina torquata* (coleopteran order, 6 cm long and weighing 12 g on average) was
156 used as the insect platform for the biological actuator. The beetle was placed on a plastic plate
157 and wrapped with dental wax for immobilization. The motion of the beetle's front leg is
158 originally with three degree-of-freedom (DoF), namely, protraction/retraction,
159 levation/depression, and extension/flexion. One DoF motion of protraction/retraction was
160 isolated by inserting two insect pin tips into the corresponding articulations to fix two other
161 joints. The motion of the beetle's front leg was thus reduced to one DoF. One antagonistic
162 pair of muscles on the back of the beetle (Figure 1A) was targeted for electrical stimulation to
163 control the isolated protraction/retraction motion of beetle's front leg with proposed fuzzy-
164 control system. Four small holes were punched on the pronotum using an insect pin. They
165 were used for two separated channels stimulating the targeted antagonistic pair of muscles.
166 Teflon-insulated thin silver wire was used as the stimulation electrode, with the inserted
167 portion flamed to remove the insulation layer. The length of the inserted portion of the
168 stimulation electrodes was maintained at 2 mm.

169 The stimulation system consisted of a control computer, a motion-detection system, and
170 a stimulation circuit (Figure 1B). The control computer used our customized software
171 BeetleCommander to control the monophasic square pulse, namely pulse-width-modulation
172 (PWM) wave, as the stimulation signal. The electrical stimulation signal was generated using
173 a custom-programmed microcontroller (Chipcon Texas Instruments CC2431, 6 × 6 mm, 130
174 mg, 32 MHz clock). The stimulation pulse width was fixed at 1 ms, and the frequency was set
175 between 0 and 200 Hz, because 200 Hz was already beyond the limitation of the beetle leg
176 levitation [20]. The stimulation voltage was fixed at 1.5 V using AA batteries. For precision
177 control of a single individual muscle, the stimulating electrical current flow was restricted to
178 only the targeted muscle. However, the biological materials used, i.e. the beetle leg muscles in
179 this case, was internally connected with shared tissue fluid. To achieve that isolation situation,
180 all stimulation channels were isolated using opto-isolators connected with individual AA
181 batteries.

182 183 *2.2. Motion-detection system.*

184 VICON[®] vision detection system was adopted for our research to gather feedback information.
185 The motion of beetle's front leg with three markers placed onsite accordingly is monitored by
186 VICON[®] 3D motion-detection system. Two markers placed on the beetle's leg were
187 recognized by the 3D motion-detection system as a solid line segment, and the third marker,
188 placed on the beetle's body, indicated the beetle's position (Figure 1C and 1D). The 3D
189 motion-detection system with 6 cameras is able to detect and store the X, Y, and Z
190 coordinates of all markers. The angular displacement was calculated using the formula for
191 angle calculation between two vectors, as follows:

192

$$\vec{P} = \begin{pmatrix} X_1 - X_2 \\ Y_1 - Y_2 \\ Z_1 - Z_2 \end{pmatrix}, \quad \vec{P}' = \begin{pmatrix} X'_1 - X'_2 \\ Y'_1 - Y'_2 \\ Z'_1 - Z'_2 \end{pmatrix}$$

193

194

$$\Delta\theta = \cos^{-1}\left(\frac{\vec{P} \cdot \vec{P}'}{|\vec{P}||\vec{P}'|}\right) \quad (1)$$

195

196 where \vec{P} is the rest neutral position vector, and \vec{P}' is the current position vector, and $\Delta\theta$ is the
 197 angle between the rest neutral position and current position vector, namely the angular
 198 displacement.

199

200

201

202

203

204

205

206

207

208

209

210

211

212

213

214

215

216

217

218

2.3. Fuzzy-Control System for electrically stimulated motion of beetle's leg muscle.

219

220

221

222

223

224

225

226

227

228

229

230

231

232

233

To achieve the utilization of large biological units in a living organism, which is suggested as a major challenge for practical use of a living machine [1], we proposed the use of a feedback-control system on the PWM wave electrical-stimulation output on the beetle's leg muscles with a fixed 1-ms pulse width and adjustable stimulation frequency. Comparing the properties of biomaterials and conventional man-made devices adopted in biohybrid robots, we suggested that a conventional PID controller is an impractical choice. On the basis of the properties of biomaterials corresponding to electrical stimulation of PWM wave, we accordingly developed a fuzzy control system with multiple membership functions, using the stimulation frequency as a single varying output to control the beetle's leg motion to precisely follow a predetermined motion path. In this paper, we consider the conventional control system with a single proportional controller as a representation. For the fuzzy-control we also proposed to adopt a proportional controller. We demonstrated that the fuzzy controller performs better than the conventional controller. Before investigating these feedback-control systems, in the following section, we characterize, in detail, the properties of the biomaterial (e.g. insect leg muscles) adopted as a large functional element under electrical stimulation.

234 Traditional man-made robotic actuators widely adopted in past, which rely on
235 mechatronics systems consisting of electrical, pneumatic or hydraulic motors, have
236 deterministic characters. The relationship between input and output is exact deterministic
237 according to physical laws and mathematical formulas, and it could be locally approximated
238 by linear functions and simplified as a time-invariant system. For example, the torque or the
239 angular acceleration generated by the electrical motor with a fixed input voltage and fixed
240 rotational speed is constant and time-invariant. The linear relationship and the time-invariant
241 system are two key presumptions for a conventional control system.

242 However, the living biological functional element does not fulfill these presumptions. The
243 inner structure of biomaterials and its chemical reactions as a driving force are yet to be
244 thoroughly studied. The reaction of the beetle leg's angular displacement corresponding to
245 electrical stimulation with a fixed frequency was generalized and empirically studied using
246 experimental data. The experimental result indicated that fuzzy control system is suitable to
247 address this issue.

248

249 2.3.1. *Graded motion control data.* Relationship between the stimulation frequency and the
250 corresponding angular displacement of the beetle's leg was well studied [20]. For the reaction
251 of angular displacement to varying stimulation frequencies in the time domain, the
252 stimulation frequency was fixed and the angular displacement of the beetle's leg was recorded
253 from its initial position to its maximum position with respect to time. For the maximum
254 angular displacement in the frequency domain, only the maximum angular displacement of
255 the beetle's leg under each fixed stimulation frequency was recorded. Statistical analysis of
256 the mean value and deviation was studied.

257 The stimulation voltage was fixed at 1.5V for all experiments (10–100 Hz, 0 to 0.5 s, N =
258 5, n = 25. Unless otherwise stated, N refers to the number of beetles used for each feedback
259 control experiment and n refers to the number of trials for overall individual beetles in this
260 paper). The electrical stimulation was applied directly on beetle's leg muscle via silver wire at
261 fixed frequency from 10 Hz to 100 Hz with 10 Hz interval. Five individual beetles were used
262 for each experiment, and each experiment of electrical stimulation at fixed frequency was
263 repeated five times.

264 The angular displacement reaction of the beetle's leg corresponding to a fixed stimulation
265 frequency (10–100 Hz, 0 to 0.5 s, N = 5, n = 25) was studied in the time domain [20]. The
266 graded motion analysis shows a strong time-dependent relationship between the electrical
267 stimulation frequency and the leg's angular displacement. The concave curve of the angular
268 displacement indicates a decreasing angular velocity with respect to time. In addition, the
269 maximum angular displacement reaction of the beetle's leg corresponding to a fixed
270 stimulation frequency (20–100 Hz, N = 5, n = 25) was studied in the frequency domain. The
271 angular displacement reached its maximum position after 0.5 s. The graded motion data also
272 shows a well-established proportional relationship between the electrical stimulation
273 frequency and the leg's angular displacement. The experiment result showed that the living
274 biological functional element is a nonlinear, time-variant system.

275 The graded motion analysis [20] indicate that the larger the difference in the stimulation
276 frequency, the larger the difference in the time required for the beetle's leg to reach the
277 maximum angular displacement position. This implies that during continuous stimulation, a
278 larger change in the stimulation frequency results in a longer time required by the beetle's leg
279 to reach the maximum angular displacement position. Moreover, only after the beetle's leg
280 reaches the maximum angular displacement position, we can gather valid feedback
281 information on the beetle leg's angular displacement by using a 3D motion-detection system.

282 Therefore, the system requires the membership function to adjust the update time interval on
283 the basis of each desired change in the output value. The update time interval is defined as the
284 total time of the current stimulation wave before the next update of the stimulation frequency.
285 It is mainly designed to be no shorter than the time that the beetle leg takes to reach its final
286 position, under a certain stimulation frequency. It can be deduced from the graded motion
287 control data [20].

288

289 *2.3.2. Hysteresis motion data.* The graded motion result only provided the relationship
290 between the stimulation frequency and the levitation angle starting from the same initial
291 position with the same initial muscle length. This hysteresis test targeted the angular
292 displacement of the beetle's front leg starting from a neutral position under electrical
293 stimulation with the stimulation frequency continuously increasing from 10 to 120 Hz, and
294 the angular displacement from the maximum angular displacement position under electrical
295 stimulation with the stimulation frequency continuously decreasing from 120 to 10 Hz.
296 Before the experiment, the leg was placed and released at rest around middle of the angular
297 displacement range without any electrical stimulation as neutral beginning position which is
298 set at zero degree. The angular displacement of the leg was measured relatively to that neutral
299 position.

300 The experiments with increasing and decreasing stimulation frequency were continuously
301 performed successively without pause. The stimulation frequency was increased from 10 to
302 120 Hz, with a 10 Hz step, and then was decreased from 120 to 10 Hz, with a 10 Hz step. The
303 stimulation at each frequency was maintained for 800 ms for the beetle's leg muscle to reach
304 its saturation position. We targeted protraction/retraction muscles, an antagonistic pair of
305 muscles, and stimulated these muscles. For example, when the protraction muscle was
306 stimulated, the retraction muscle was reserved intact (no stimulation) so that the retraction
307 muscle did not exert force on the joint and the induced angular displacement was solely due
308 to the electrical stimulation of the protraction.

309 The angular displacement with increasing and decreasing stimulation frequency (10–120
310 Hz, N = 5, n = 25) demonstrated that the targeted biomaterial, namely the beetle's leg-muscle
311 tissue, exhibits strong hysteresis property. The detailed data gathered in the experiment was
312 thoroughly studied with statistics in the following results section.

313

314 *2.3.3. Theoretical analysis of conventional control system with a single proportional*
315 *controller.* We adopted a conventional control system with a single proportional controller as
316 a representation of a conventional control system. A conventional control system with a
317 single proportional controller is theoretically equivalent to a fuzzy control system with a
318 single membership function. The experimental results of the single proportional controller
319 system were gathered for further study of general properties of the proportional controller.
320 The effect of the membership function on the fuzzy control system was studied and revealed
321 on the basis of the results, which were used for preparing the fuzzy control system designed
322 with multiple membership functions.

323 The concept of proportional control was used to adjust the magnitude of the step
324 increment and decrement of the stimulation frequency according to the following function:

$$325 \quad f_{out}^* = f_{out} + K_p \times e(t) \quad (2)$$

326 where

327 f_{out} is the last output stimulation frequency from the proportional controller.

328 f_{out}^* is the updated output stimulation frequency from the proportional controller.

329 K_p is the proportional gain (adjustable by user).
330 $e(t)$ is the instantaneous angular displacement error at time t .
331 The initial output stimulation frequency was set to 2 Hz, and a maximum ceiling of 120 Hz
332 was adopted for the output stimulation frequency. The graded motion data and the hysteresis
333 graph demonstrated that the effect of the stimulation frequency below 2 Hz is basically
334 negligible, and that the leg angular displacement reaches its maximum motion range with the
335 stimulation frequency beyond 120 Hz (Figure 2). The minimum frequency for levitation
336 stimulation is 2 Hz, which means there is always stimulation for the levitation leg muscle.
337 The minimum frequency for counterpart stimulation is 0 Hz, which means there can be no
338 stimulation for the counterpart leg muscle.

339 The electrical stimulation frequency from one channel initially increased to elicit the leg
340 to move to the desired position. If the actual leg motion angle became larger than the
341 predefined angle, the stimulation from the current working channel continued to decrease its
342 stimulation frequency, whereas the stimulation from the counter-channel started decreasing
343 the motion angle by increasing the corresponding stimulation frequency. Similarly, if the
344 actual motion angle became smaller than the predefined angle, the counter-channel stopped
345 generating the stimulation signal and the previous working channel started to increase its
346 stimulation frequency to increase the leg motion angle. As such, the two channels that
347 stimulated the antagonistic pair of muscles worked simultaneously to ensure that the beetle's
348 leg followed the predetermined motion path.

349 The detected angle displacement, the desired angle displacement, and their difference
350 were used as the input parameters. The proportional gain of the controller and the update time
351 interval were used as the output parameters. On the basis of the analysis of the results from
352 the conventional control system with a single proportional controller, the relationship between
353 the input and output parameters was well studied. The membership function of the fuzzy
354 control system changed both the value of proportional gain and the update time interval to
355 account for the angular motion of the leg. The fuzzy control system with multiple
356 membership functions was designed in accordance with our findings on the relationship
357 between these two key factors and the experiment results.

358
359 *2.3.4. Theoretical analysis of fuzzy control system with multiple membership functions.* A
360 fuzzy control system conceptually consists of three stages. An input stage, which reads
361 feedback sensor values and then maps sensor or other inputs to the appropriate membership
362 functions; a processing stage, which invokes the predefined membership functions and then
363 calculates the result; and an output stage, which converts the result from the processing stage
364 into a specific control output value. For the output stage, we used a proportional controller for
365 the feedback control system. For the processing stage, we used the membership function to
366 adjust the proportional gain of the controller and other parameters of the control system.

367 In the input stage, the input parameters include the detected angular displacement, and
368 desired angle displacement. These two parameters are mapped to the appropriate membership
369 functions. The proposed shape of the membership functions is triangular. We selected the
370 same point as the start and end of each detected angle displacement for the triangular
371 membership functions. Consequently, each detected angle displacement had one unique
372 corresponding membership function. As a result, at each detected angle displacement, the
373 membership function gives one unique proportional gain for the output stage.

374 On the basis of the relationships between the key factors and the feedback control results,
375 the corresponding membership functions could be designed as follows:

376 (a) The system adopts a larger proportional gain for a larger angle difference between the
 377 detected and desired angle displacements. Proportional gain also increases with a larger
 378 desired angle input. Two variables as input, namely the angular difference between the
 379 detected and desired angular displacements $|\theta_{Desired} - \theta_{Current}|$, and the desired angular
 380 displacement $\theta_{Desired}$, and one dependent variable, namely K_p^* , as output are for the
 381 membership function. For simplicity, efficiency, reliability, and general applicability, we
 382 adopted a linear relationship of the increase in proportional gain. No other relationship is
 383 justified theoretically to have better performance than a simple linear relationship. It has the
 384 general linear relation form between the input and output as $Y = \beta_0 + \beta_1 X_1 + \beta_2 X_2$,
 385 according to the function below.

$$386 \quad K_p^* = K_{p_{base}} + a_{K_p} \times |\theta_{Desired} - \theta_{Current}| + b_{K_p} \times \theta_{Desired} \quad (3)$$

387 K_p^* is the P controller value for the next frequency update

388 $\theta_{Desired}$ is the desired angle of motion used as the input

389 $\theta_{Current}$ is the current angle of motion detected by the VICON[®] 3D system

390 $K_{p_{base}}$, a_{K_p} , and b_{K_p} are parameters

391 $K_{p_{base}} + a_{K_p} \times |\theta_{Desired} - \theta_{Current}|$ is the linear relationship between proportional gain
 392 and angle difference

393 $b_{K_p} \times \theta_{Desired}$ is the increase in proportional gain from a larger desired angle input

394 (b) The system adopts a longer update time interval for a larger angle difference between the
 395 detected and desired angle displacements. The update time interval also increases with a
 396 larger desired angle displacement. For the same reason and in the same form as K_p^* , we
 397 adopted a linear relationship for the membership function of T^* , according to the function
 398 below.

$$399 \quad T^* = T_{base} + a_T \times |\theta_{Desired} - \theta_{Current}| + b_T \times \theta_{Desired} \quad (4)$$

400 T^* is the update time interval for the next frequency update

401 $\theta_{Desired}$ is the desired angle of motion used as the input

402 $\theta_{Current}$ is the current angle of motion detected by the VICON[®] 3D system

403 T_{base} , a_T , and b_T are parameters

404 $T_{base} + a_T \times |\theta_{Desired} - \theta_{Current}|$ is the linear relationship between update time interval
 405 and angle difference

406 $b_T \times \theta_{Desired}$ is the increase in update time interval from a larger desired angle input

407 The membership function parameters include proportional gain and update time interval,
 408 which are determined by the angle difference and desired angle displacement according to
 409 functions (3) and (4), respectively. The processing stage invokes the unique corresponding
 410 membership function, and generates the corresponding stimulation frequency and the update
 411 time interval according to function (2). Finally, in the output stage, the microcontroller
 412 converts the stimulation frequency and update time interval into corresponding PWM waves.

413 For the hysteresis properties of the beetle's leg muscle under electrical stimulation, we
 414 generally consider that the corresponding stimulation frequency of a certain angular
 415 displacement is in a fuzzy status. Considering the motion direction of the beetle's leg, we can
 416 narrow this fuzzy status into a smaller range of frequencies according to the hysteresis
 417 property graph shown in Figure 2. Such additional modules, e.g., adding binary factors of
 418 motion direction into equation (3), may improve the fuzzy control system in theory for future
 419 development.

420

421 2.4. Experimental setup

422 The first set of experiments was performed using the conventional control system with a
423 single proportional controller to achieve a preset angular displacement of 20° . We adopted a
424 conventional control system with a single proportional controller having proportional gain
425 values ranging from 0.5 to 1.0, with 0.1 increments.

426 The second set of experiments was performed using a fuzzy control system with multiple
427 membership functions to achieve a preset angular displacement of 20° . Individual beetles
428 same as those used in the conventional control system were tested for this experiment.

429 From the result of the first set of experiments, which used conventional control system,
430 we deduced the lower and upper bounds for the value of proportional gain, as well as the
431 update time interval for each value of proportional gain, and hence established a linear
432 relationship between the update P controller proportional gain value and the update time
433 interval.

434 K_p values are adjusted according to equation (3), where K_p^* represents the real-time
435 calculated K_p value for the proportional controller. There are two types of parameters. The
436 first are user input parameters, namely $\theta_{Desired}$, b_{K_p} , the calibration value 1 and 2 for K_p
437 with corresponding value 1 and 2 for $|\theta_{Desired} - \theta_{Current}|$. The second are values calculated
438 from calibration, namely $K_{p_{base}}$, a_{K_p} . Before the experiment, the user inputs the values of the
439 user input parameters based on conclusions from previous experiments. Our previous
440 experiment showed that the proportional gain should be larger than 0.5 and smaller than 1 in
441 order to have the closed-loop control work in practice. When the proportional gain was
442 smaller than 0.5, the beetle's leg did not reach the predetermined position. When the
443 proportional gain was larger than 1, the fluctuation did not settle at the predetermined path.
444 The largest absolute angular displacement range was around 40 degree for both upward and
445 downward movements, which depended on both the experiment setup and individual beetle
446 [20]. We use these values as boundary conditions. The proportional gain $K_p^* = 1.0$ is
447 corresponding to the largest angular difference $|\theta_{Desired} - \theta_{Current}| = 40$. The proportional
448 gain $K_p^* = 0.6$ is corresponding to the angular difference $|\theta_{Desired} - \theta_{Current}| = 5$. The
449 parameter $b_{K_p} = 0.02$ is empirically optimized from our experiment result. These values were
450 empirically optimized values from various experiment to have our presented experiment
451 result.

452 After that, we use calibration, according to the following conditions 1 and 2.

453 $K_p^* = 1.0$ according to equation (3) when $|\theta_{Desired} - \theta_{Current}| = 40$ (Condition 1)

454 $K_p^* = 0.6$ according to equation (3) when $|\theta_{Desired} - \theta_{Current}| = 5$ (Condition 2)

455 to calculate the values for the rest of the parameters $K_{p_{base}}$ and a_{K_p} . We have two
456 unknown parameters in equation (3). We have to conditions to calculate the unknown
457 parameters.

458 T_p values are adjusted according to equation (4) in the same way as K_p in equation (3).
459 The values of four parameters are also obtained in the same way as for the K_p in equation (3)
460 based on our previous experiment result [20]. Before the experiment, the user inputs the
461 values of the user input parameters based on conclusions from previous experiments. Our
462 empirically optimized result is that the largest update time interval $T^* = 400$ is corresponding
463 to the largest angular difference $|\theta_{Desired} - \theta_{Current}| = 40$. The update time interval
464 $T^* = 100$ is corresponding to the angular difference $|\theta_{Desired} - \theta_{Current}| = 5$. The
465 parameter $b_T = 1$ is empirically optimized from our experiment result.

466 After that, we use calibration, according to the following conditions 3 and 4.

467 $T^* = 400$ according to equation (3) when $|\theta_{\text{Desired}} - \theta_{\text{Current}}| = 40$ (Condition 3)
468 $T^* = 100$ according to equation (3) when $|\theta_{\text{Desired}} - \theta_{\text{Current}}| = 5$ (Condition 4)
469 to calculate the values for the rest of the parameters T_{pbase} and a_T . We have two unknown
470 parameters in equation (4). We have to conditions to calculate the unknown parameters.

471 During the experiment, we have feedback of the current angular displacement θ_{Current} .
472 With all the values of the parameters known, we can thus calculate the values of K_p^* and T^*
473 accordingly.

474

475 *2.5. Hardware implementation of the fuzzy control system.*

476 We developed customized software BeetleCommander for the fuzzy feedback control system.
477 Electrical stimulation signals generated from two separate stimulation channels were used to
478 control one antagonistic pair of muscles. BeetleCommander extracted instantaneous marker-
479 position information from the 3D motion-detection system and calculated the immediate leg-
480 motion angle. The protraction/retraction feedback motion control was adopted as an example
481 to explain the working principle of our feedback control system, which was controlled by two
482 separate channels from BeetleCommander. Electrical stimulation signals from the two
483 channels were automatically generated according to the desired motion angle/path input. Both
484 channels of stimulations worked independently and concurrently.

485 For the fuzzy control system, the input consisted of three parameters: the detected angle
486 displacement from the 3D motion-detection system, the user input desired angle displacement,
487 and the angle difference between the detected and desired angles. The output comprised two
488 parameters: the output frequency for the PWM wave and the update time interval.

489 The graded motion control results show the minimum time required to reach the
490 maximum angular displacement position with respect to the stimulation frequency. The
491 relationship between the minimum time required, namely the update time interval, and the
492 stimulation frequency is nondeterministically proportional. Together with the hysteresis test
493 results, the data show that the relationship between the angular displacement and the
494 stimulation frequency is also nondeterministically proportional. For ease of implementation,
495 we simplified these nondeterministically proportional relationships into proportional
496 relationships using adjustable parameters.

497 The output frequency of the fuzzy control system was non-integer because of the non-
498 integer feedback data and non-integer proportional controller gain. For the convenience of
499 electrical stimulation with no measurable difference, we used all integer values for the output
500 stimulation frequency. To achieve that, we replaced the output frequency with its nearest
501 integer number.

502

503 *2.6. Data analysis and statistics.*

504 In the data analysis of the experiments described herein, N refers to the number of beetles
505 used for each feedback control experiment and n refers to the number of trials for overall
506 individual beetles. Values are given as mean \pm standard deviation. Overshoot was calculated
507 as absolute angular displacement as well as in percentage form. The mean overshoot, as well
508 as the mean reaching time, was calculated as an average over n number of trials.

509

510

511 **3. Results and Discussion**

512 *3.1. Muscle reaction to electrical stimulation is a nonlinear, time-variant system with*
513 *hysteresis property.*

514 The hysteresis motion data in Figure 2 indicate that for the same difference in angular
515 displacement, the difference in the stimulation frequency is large when the absolute angular
516 displacement is very large or very small, approximately above 25° or below 15° , and that the
517 difference in the stimulation frequency is small when the absolute angular displacement lies
518 in the middle range, from approximately 15 to 25 Hz. Consequently, a fast change in the
519 stimulation frequency is required when the absolute angular displacement is very large or
520 very small, and a slow change in the stimulation frequency is required when the absolute
521 angular displacement is in the middle range. Such a property does not exist in a time-invariant
522 linear system. Thus, to realize this preferred result, the system must adopt membership
523 functions to adjust the controller parameters, mainly the proportional gain for a proportional
524 controller, on the basis of the feedback information.

525 Results in the frequency domain, shown in Figure 2, indicated that when the beetle's leg
526 moves away from the neutral position, the stimulation frequency increases slowly at the
527 beginning and then rapidly for the same increase in angular displacement, while in case of
528 movement toward the neutral position, the stimulation frequency decreases slowly at the
529 beginning and then rapidly for the same decrease in angular displacement. To reach the same
530 angular displacement, the corresponding frequency of the motion type moving toward the
531 neutral position differs from that of the motion type moving away from the neutral position.

532 Because a significant difference exists in the stimulation frequencies required to reach
533 the same angular displacement between the movement away from and the neutral position and
534 that toward it (Figure 2), the detected angular displacement does not clearly indicate the exact
535 corresponding value of the stimulation frequency. For example, 80 Hz was considered as
536 higher stimulation frequency with larger angular displacement for the movement away from
537 the neutral position, with corresponds to an approximately 25° angular displacement. On the
538 other hand, 60 Hz was considered as the higher stimulation frequency with larger angular
539 displacement for the movement toward the neutral position, which corresponds to an
540 approximately 30° angular displacement.

541 The deviation in the angular displacement is much smaller for the increasing stimulation
542 frequency as compared with that for the decreasing stimulation frequency. The deviation is
543 accumulative because the experiment is continuously ongoing with variable stimulation
544 frequency. Furthermore, the electrical stimulation effect with varying frequency has minimum
545 and maximum limitations, which depend on the beetle's own properties and are unique for
546 each beetle; yet they are, in general, approximately 20 Hz and 100 Hz, respectively (Figure 2).
547 The proportional relationship between the stimulation frequency and swinging angular
548 displacement was effectively established only on a partial span of the entire simulation
549 frequency.

550 We considered the above mentioned properties, and the fact that the internal biological
551 working mechanism and chemical reaction of beetle muscle is difficult to be mathematically
552 modeled. Thus, we reached the conclusion that a simplified linearized relationship between
553 the stimulation frequency and angular displacement, angular velocity, or angular acceleration
554 of the leg motion is not able to be established in practice. Those three parameters of the leg
555 motion are also strongly dependent on reaction time, which was demonstrated in the graded
556 motion data [20] and Figure 2.

557 These results conclude that the biomaterial of insect muscle tissues is a nonlinear and
558 time-variant system. And the experiment result showed that the living biological functional
559 element exhibits an unclearly defined fuzzy relationship between the electrical stimulation
560 frequency and angular displacement of the beetle's leg.

561

562 3.2. Both conventional and fuzzy control systems can steer the insect leg to follow a
563 predetermined path, but the latter performs better.

564 On the basis of the relationship between the electrical stimulation frequency and the beetle
565 leg's angular displacement, we used the concept of fuzzy control to steer the leg movement
566 according to a preset angular displacement and hence follow a predetermined motion path,
567 which was separated into a series of consecutive preset angular displacements. Figure 3A and
568 3B shows the schematic representation of both conventional and fuzzy control systems.

569 The conventional control system with a single proportional controller was adopted for
570 the experiment ($\pm 20^\circ$ step function, $t = 10$ s, $N = 5$, $n = 30$). Figure 4 demonstrates that such a
571 control system can enable the beetle's leg motion to follow the preset angular displacement
572 closely. With an increment in the proportional gain of the controller (K_p) from 0.5 to 1.0, the
573 leg response overshoot generally increases, whereas the settling time decreases. The fuzzy
574 control system with multiple membership functions was adopted for the experiment ($\pm 20^\circ$
575 step function, $t = 10$ s, $N = 5$, $n = 30$). Figure 5A demonstrates that the fuzzy control system
576 can also enable the beetle's leg motion to follow the preset angular displacement closely. It
577 also shows the stimulation frequency in the corresponding time domain.

578 Three major properties of the two control systems—overshoot displacement, reaching
579 time, and damping effect—were compared. Figure 5B illustrates how the values of overshoot
580 displacement and reaching time were determined. The overshoot displacement is defined as
581 the first peak value of the detected motion path. Because the beetle is alive and can steer its
582 own legs' angular displacement, we selected the first peak value to avoid extreme cases where
583 the first peak value as overshoot is not the maximum value. The reaching time is defined as
584 the time between the change in the desired input angle and the first reach of the desired angle
585 of the beetle's leg. The living functional element may not settle into the predetermined path
586 but rather fluctuate around it because of the internal noise from the beetle's own movement.
587 Thus, with such a possibility, the reaching time is a significant indicator of the system's
588 response rate. The damping effect is defined as the fluctuation in the beetle leg's angular
589 displacement around the predetermined path.

590 The controlled leg movement exhibits the following three interesting properties. (1) The
591 overshoot angular displacement. (2) The reaching time, instead of settling time, which is the
592 time span between the start of the input angle and the first time the system reaches the input
593 angle; because of the obvious fuzzy system property and disturbance from the beetle itself,
594 the settling time may not accurately reflect the system's response time, or there may not even
595 be a settling time because of the fluctuation. (3) The damping effect, which is the fluctuation
596 in the controlled motion.

597 On the basis of the above presented experimental results in Figure 5A, we conclude as
598 follows: With increasing proportional gain, the experimental results demonstrate decreasing
599 steady-state error, decreasing reaching time, and increasing damping and increasing overshoot.
600 With increasing update time interval, the experimental results demonstrate decreasing
601 damping and increasing reaching time.

602 The fuzzy control system with multiple membership functions minimizes these
603 disadvantages and has the closest control fit for the predetermined leg motion path. Figure 6A
604 and 6B show a statistical analysis of the comparison of the overshoot and reaching time
605 between a conventional controller with a single proportional controller and a fuzzy control
606 system with multiple membership functions. For the conventional control system, the graphs
607 show the effect of proportional gain on the overshoot and reaching time, as well as the result
608 of the fuzzy control system with multiple member functions. Table 1 shows the detailed
609 values of the statistical analysis. The overshoot increases with the proportional gain of the

610 conventional controller to a certain point, approximately $p = 0.9$, while the fuzzy system with
611 multiple membership functions exhibits the smallest overshoot. The reaching time for the
612 conventional control system decreases with increasing proportional gain, while the fuzzy
613 control system with multiple membership functions exhibits well averaged reaching time.
614 Comparing Figure 4 and 5A, we conclude that the damping increases with the proportional
615 gain, and the fuzzy system with multiple membership functions exhibits the modest damping.

616 For the fuzzy control system, the internal parameters that cause the decrease in overshoot
617 lead to an increase in reaching time, which is in accordance with the intrinsic property of the
618 proportional controller. Although the fuzzification function changes the parameters, the fuzzy
619 control system with multiple membership functions still adopts the proportional controller for
620 the control loop. The decrease in overshoot requires smaller proportional gain—which leads
621 to lower system response, i.e., longer reaching time. By tuning the membership function of
622 fuzzification, i.e., by varying the values of the fuzzification function parameters, the desired
623 balance between system overshoot and reaching time can be achieved.

624

625

626 **4. Conclusion**

627 [Toward an insect leg actuator based on electrical stimulation of leg muscles, a fuzzy](#)
628 [control system with multiple membership functions was developed and demonstrated](#)
629 [to regulate a beetle's leg to follow a predetermined motion path. The hysteresis was](#)
630 [found in the proportional correlation between the frequency of the muscle electrical](#)
631 [stimulation and the angular displacement of the stimulated leg. For that, instead of the](#)
632 [conventional proportional control system, the fuzzy control system was adopted to](#)
633 [regulate the angular displacement and it achieved a smaller overshoot, shorter](#)
634 [reaching time, and less damping effect of fluctuation.](#)

635

636

637 **Acknowledgements**

638 This work has been supported by Nanyang Assistant Professorship (NAP), Agency for
639 Science, Technology and Research (A*STAR) Public Sector Research Funding (PSF), and
640 A*STAR-JST (The Japan Science and Technology Agency) joint grant. The authors offer
641 their appreciation to Mr. Chew Hock See, Mr. Cheo Hock Leong, Mr. Ow Yong See Meng,
642 Ms. Chia Hwee Lang, Mr. Roger Tan Kay Chia at School of MAE, NTU. The authors thank
643 Professor Pieter Abbeel (UC Berkeley), Professor Kazuo Ikeda (City of Hope Medical
644 Center), and Professor Michel M. Maharbiz (UC Berkeley) for their helpful advice, and
645 Professor Kris Pister (UC Berkeley) for providing the wireless communication device.

646

647 **Author contributions**

648 CZ, FC, TTVD, YL and HS designed research, CZ, FC and HS performed research; CZ, FC
649 and HS analyzed data; CZ, FC and HS wrote the paper.

650

651

652 **Additional Information**

653 Competing financial interests: The authors declare no competing financial interests.

Figure Legends

Figure 1. Experiment materials and devices. (A) Anatomical view of the protraction/retraction pair of muscles controlling the front leg's angular motion. The positions of the implanted stimulation electrodes, namely thin silver wires, are indicated by red crosses. (B) The hardware setup for the closed-loop control system and the 3D motion-detection system. A laptop with a circuit board is used for the closed-loop control system. One desktop with camera sets is used as the 3D motion-detection system. (C) The positions of the markers placed on the beetle, which are recognized by the 3D motion-detection system as point objects. (D) The representation of the recognized markers on the 3D motion detection system. The femur–tibia section of the beetle's leg is represented by the solid line segment joining the two markers placed on the front leg. The lower point indicates the body of the beetle.

Figure 2. Hysteresis motion of electrically stimulated insect-leg. Hysteresis motion for angular displacement corresponding to different stimulation frequencies of two motion types—movement toward and movement away from the neutral position predefined manually ($N = 5$, $n = 25$). The stimulation frequency starting from 10 Hz is continuously increased to 120 Hz and continuously decreased to 10 Hz, with a 10 Hz step. The stimulation remains at each stimulation frequency for 800 ms. (A) and (B) are reproduction from the authors' previous work in [20] with permission under the terms of the Creative Commons Attribution License in that journal.

Figure 3. Schematic representation of the fuzzy control system. (A) Schematic representation of the fuzzy control system with a single membership function, which is a proportional controller. Instantaneous marker positions are used as the system's feedback information input for adjusting the stimulation frequency as the system's output. (B) Schematic representation of the fuzzy control system with multiple membership functions. Each membership function is a proportional controller. Instantaneous marker positions are used as the system's feedback information input.

Figure 4. Result of conventional control system with single proportional controller. The comparison between the actual leg motion path (red line) and predetermined motion path (blue line). As the K_p value increases, the leg response overshoot generally increases, whereas the settling time decreases ($N = 5$, $n = 35$).

Figure 5. Result of fuzzy control system with multiple membership functions. (A) The comparison between the actual leg motion path (red line) and the predetermined motion path (blue line). The stimulation frequency of two stimulation channels is presented in the same time line as the angular displacement graph ($N = 5$, $n = 35$). (B) Fuzzy controller data result example demonstrates how we interpret the presented experimental data. Overshoot and reaching time are defined accordingly.

Figure 6. Comparison of overshoot and reaching time between fuzzy control and conventional control. (A) The graphs provide statistical analysis of the overshoot results in both absolute angle displacement and percentage ($N = 5$, $n =$

35). The blue bar graph indicates the average value, and the error indicates the deviation. The first blue bar graph shows the result of the fuzzy system with multiple membership functions. The blue bar graphs after the first one show the result of the fuzzy system with a single membership function at each K_p value from repeated experiments. (B) The graph provides statistical analysis of the reaching time results in millisecond ($N = 5$, $n = 35$). The blue bar graph indicates the average value, and the error indicates the deviation. The first blue bar graph shows the result of the fuzzy system with multiple membership functions. The blue bar graphs after the first one show the result of the fuzzy system with a single membership function at each K_p value from repeated experiments.

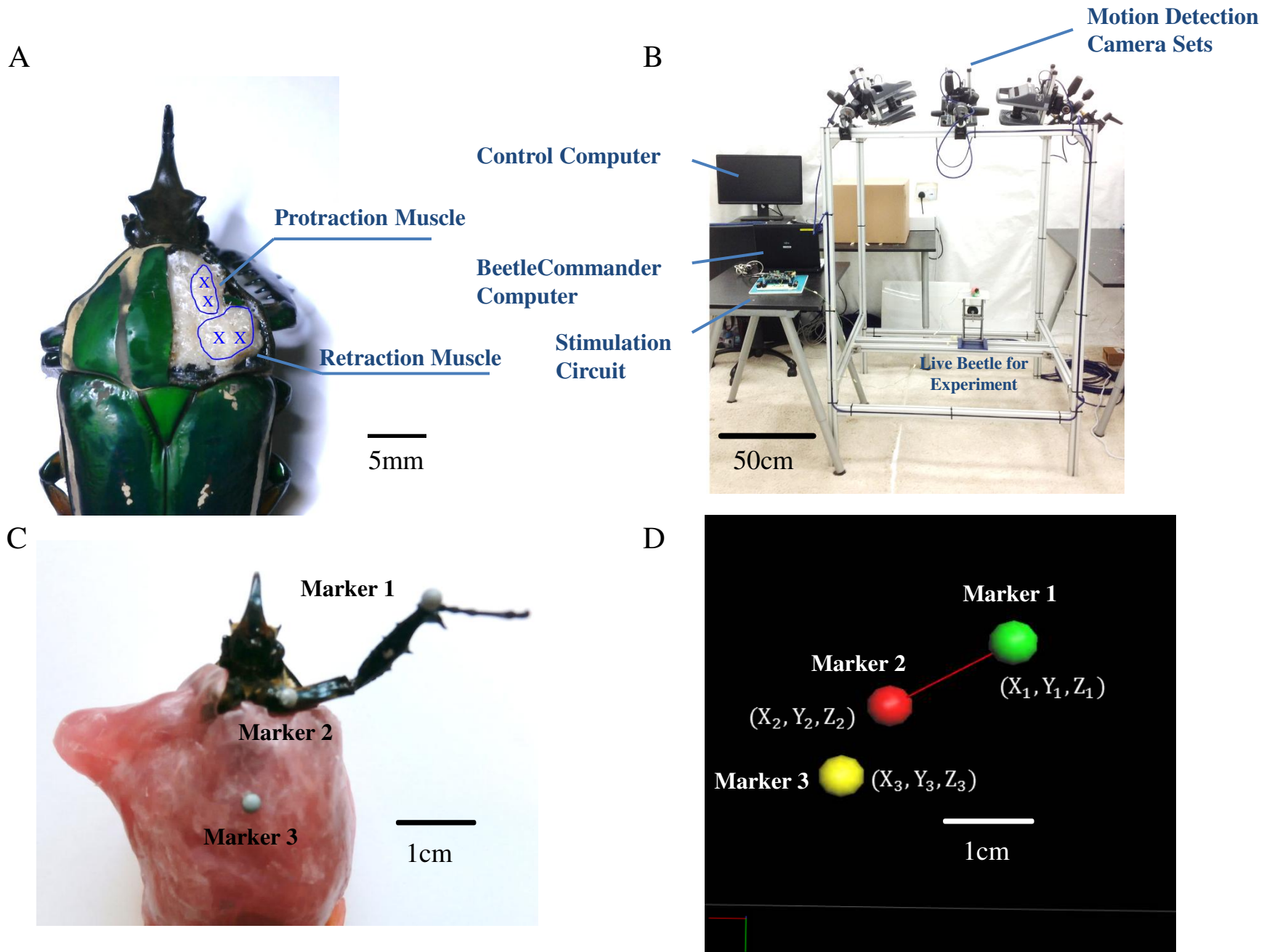
References

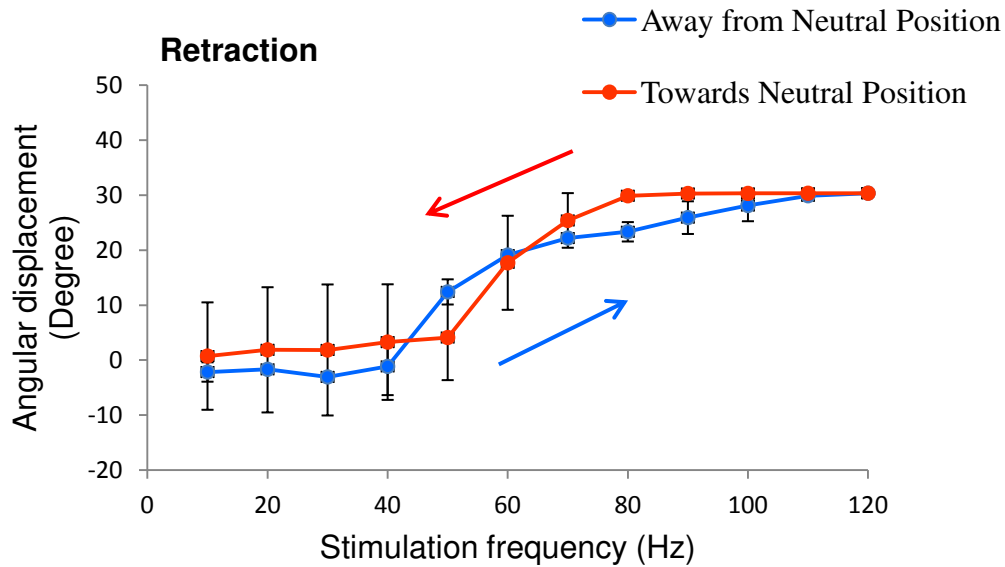
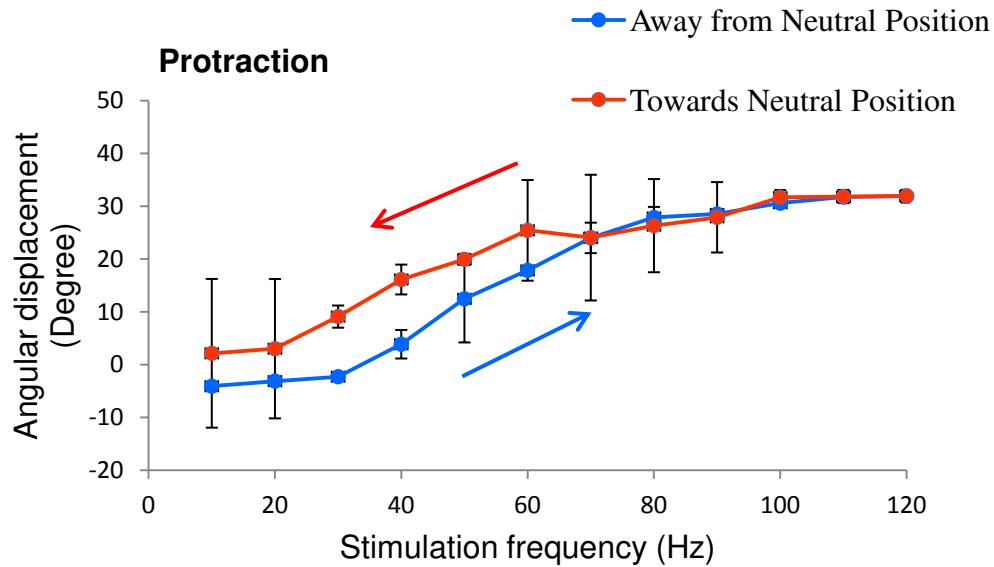
1. Gross, M., *Towards living machines*. Current biology : CB, 2013. **23**(18): p. R821-R823.
2. Akiyama, Y., et al., *Room temperature operable autonomously moving bio-microrobot powered by insect dorsal vessel tissue*. PLoS One, 2012. **7**(7): p. e38274.
3. Altendorfer, R., et al., *RHex: A Biologically Inspired Hexapod Runner*. Autonomous Robots, 2001. **11**(3): p. 207-213.
4. Bozkurt, A., J. F. Gilmour R, and A. Lal, *Balloon-assisted flight of radio-controlled insect biobots*. IEEE Trans Biomed Eng, 2009. **56**(9): p. 2304-7.
5. Daly, D.C., et al., *A Pulsed UWB Receiver SoC for Insect Motion Control*. IEEE Journal of Solid-State Circuits, 2010. **45**(1): p. 153-166.
6. Hinterwirth, A.J., et al., *Wireless stimulation of antennal muscles in freely flying hawkmoths leads to flight path changes*. PLoS One, 2012. **7**(12).
7. Holzer, R. and I. Shimoyama. *Locomotion control of a bio-robotic system via electric stimulation*. in *Intelligent Robots and Systems, 1997. IROS '97., Proceedings of the 1997 IEEE/RSJ International Conference on*. 1997.
8. Sato, H., et al., *Remote radio control of insect flight*. Front Integr Neurosci, 2010. **3**.
9. Tsang, W.M., et al., *Flexible split-ring electrode for insect flight biasing using multisite neural stimulation*. IEEE Trans Biomed Eng, 2010. **57**(7): p. 1757-64.
10. Tubbs, T.B., A.N. Palazotto, and M.A. Willis, *Biological Investigation of Wing Motion of the Manduca Sexta*. International Journal of Micro Air Vehicles, 2011. **3**(2): p. 101-118.
11. Wang, H., N. Ando, and R. Kanzaki, *Active control of free flight manoeuvres in a hawkmoth, Agrius convolvuli*. J Exp Biol, 2008. **211**(Pt 3): p. 423-32.
12. Wessnitzer, J. and B. Webb, *Multimodal sensory integration in insects--towards insect brain control architectures*. Bioinspir Biomim, 2006. **1**(3): p. 63-75.
13. Cheng, B., X. Deng, and T.L. Hedrick, *The mechanics and control of pitching manoeuvres in a freely flying hawkmoth (Manduca sexta)*. J Exp Biol, 2011. **214**(Pt 24): p. 4092-106.
14. Maharbiz, M.M. and H. Sato, *Cyborg Beetles*. Scientific American, 2010. **303**(6): p. 94-99.
15. Sato, H., et al., *A cyborg beetle: Insect flight control through an implantable, tetherless microsystem*. Mems 2008: 21st Ieee International Conference on Micro Electro Mechanical Systems, Technical Digest, 2008: p. 164-167.
16. Sato, H., et al., *Deciphering the Role of a Coleopteran Steering Muscle via Free Flight Stimulation*. Current Biology, 2015. **25**(6): p. 798-803.
17. Sato, H., et al., *Cyborg Beetles: The Remote Radio Control of Insect Flight*. 2010 Ieee Sensors, 2010: p. 1-4.
18. Sato, H., et al., *Radio-Controlled Cyborg Beetles: A Radio-Frequency System for Insect Neural Flight Control*. Ieee 22nd International Conference on Micro Electro Mechanical Systems (Mems 2009), 2009: p. 216-219.
19. Thang, V.D.T., et al., *Insect-Machine Hybrid System*. 2013 35th Annual International Conference of the Ieee Engineering in Medicine and Biology Society (Embc), 2013: p. 2816-2819.
20. Cao, F., et al., *A biological micro actuator: graded and closed-loop control of insect leg motion by electrical stimulation of muscles*. PLoS ONE, 2014. **9**(8): p. e105389.
21. Marzullo, T.C. and G.J. Gage, *The SpikerBox: a low cost, open-source bioamplifier for increasing public participation in neuroscience inquiry*. PLoS One, 2012. **7**(3): p. e30837.
22. Feng, C., et al. *Insect-machine hybrid robot: Insect walking control by sequential electrical stimulation of leg muscles*. in *Robotics and Automation (ICRA), 2015 IEEE International Conference on*. 2015.

23. Brown, A.K. and Y. Lu. *Performance test results of an integrated GPS/MEMS inertial navigation package*. in *Proceedings of ION GNSS*. 2004.
24. Chowdhary, G., et al. *Low Cost Guidance, Navigation, and Control Solutions for a Miniature Air Vehicle in GPS Denied Environments*. in *Proceedings of 1st Symposium on Indoor Flight Issues, Mayaguez, Puerto Rico*. 2009.
25. Lijie, Z. and C. Ji, *MEMS-Based Attitude Measurement System for Miniature Air Vehicle [J]*. *Journal of Vibration, Measurement & Diagnosis*, 2010. **6**: p. 026.
26. SHI, S.-h., et al., *Design of miniature electronic compass based on GMR sensor*. *Journal of Mechanical & Electrical Engineering*, 2012. **6**: p. 006.
27. Tanenhau, M., et al. *Accurate real time inertial navigation device by application and processing of arrays of MEMS inertial sensors*. in *Position Location and Navigation Symposium (PLANS), 2010 IEEE/ION*. 2010. IEEE.
28. Wei-zheng, L.A.-p.Y. and C. Hong-long, *Study on Miniature Navigation System Based on MIMU*. *Journal of Projectiles, Rockets, Missiles and Guidance*, 2005: p. S2.
29. Chen, M., et al., *Body area networks: A survey*. *Mobile networks and applications*, 2011. **16**(2): p. 171-193.
30. Latré, B., et al., *A survey on wireless body area networks*. *Wireless Networks*, 2011. **17**(1): p. 1-18.
31. Liu, J., et al., *Optical receiver front end for optically powered smart dust*. *International Journal of Circuit Theory and Applications*, 2014.
32. Scott, M.D., B.E. Boser, and K.S. Pister, *An ultralow-energy ADC for smart dust*. *Solid-State Circuits, IEEE Journal of*, 2003. **38**(7): p. 1123-1129.
33. Seo, D., et al., *Model validation of untethered, ultrasonic neural dust motes for cortical recording*. *Journal of neuroscience methods*, 2015. **244**: p. 114-122.
34. Warneke, B., et al., *Smart dust: Communicating with a cubic-millimeter computer*. *Computer*, 2001. **34**(1): p. 44-51.
35. Akiyama, Y., et al., *Culture of insect cells contracting spontaneously; research moving toward an environmentally robust hybrid robotic system*. *J Biotechnol*, 2008. **133**(2): p. 261-6.
36. Akiyama, Y., et al., *Long-term and room temperature operable bioactuator powered by insect dorsal vessel tissue*. *Lab Chip*, 2009. **9**(1): p. 140-4.
37. Sato, H. and M.M. Maharbiz, *Recent developments in the remote radio control of insect flight*. *Front Neurosci*, 2010. **4**: p. 199.
38. Guschlbauer, C., H. Scharstein, and A. Bueschges, *The extensor tibiae muscle of the stick insect: biomechanical properties of an insect walking leg muscle*. *J Exp Biol*, 2007. **210**(6): p. 1092-1108.
39. Burns, M.D. and P.N.R. Usherwood, *Mechanical properties of locust extensor tibiae muscles*. *Comparative Biochemistry and Physiology Part A: Physiology*, 1978. **61**(1): p. 85-95.
40. Debrodt, B. and U. Bassler, *Responses of flexor motor neurons to stimulation of the femoral chordotonal organ of the phasmid extatosoma-tiaratum*. *Zoologische Jahrbucher-Abteilung Fur Allgemeine Zoologie Und Physiologie Der Tiere*, 1990. **94**(1): p. 101-119.
41. de Haan, A., *The influence of stimulation frequency on force-velocity characteristics of in situ rat medial gastrocnemius muscle*. *Experimental Physiology*, 1998. **83**(1): p. 77-84.
42. Buschges, A., et al., *Synaptic drive contributing to rhythmic activation of motoneurons in the deafferented stick insect walking system*. *Eur J Neurosci*, 2004. **19**(7): p. 1856-62.

43. Malamud, J.G. and R.K. Josephson, *Force velocity relationships of a locust flight-muscle at different times during a twitch contraction*. Journal of Experimental Biology, 1991. **159**: p. 65-87.
44. Stevenson, R.D. and R.K. Josephson, *Effects of operating frequency and temperature on mechanical power output from moth flight-muscle*. Journal of Experimental Biology, 1990. **149**: p. 61-78.
45. Abdulla, S.C., O. Sayidmarie, and M.O. Tokhi, *Functional electrical stimulation-based cycling assisted by flywheel and electrical clutch mechanism: A feasibility simulation study*. Robot. Auton. Syst., 2014. **62**(2): p. 188-199.
46. Brend, O., C. Freeman, and M. French, *Multiple-Model Adaptive Control of Functional Electrical Stimulation*. Control Systems Technology, IEEE Transactions on, 2015. **23**(5): p. 1901-1913.
47. Liao, Y.W., et al., *Modeling open-loop stability of a human arm driven by a functional electrical stimulation neuroprosthesis*. Conf Proc IEEE Eng Med Biol Soc, 2013. **2013**: p. 3598-601.
48. Lynch, C.L., D. Sayenko, and M.R. Popovic, *Co-contraction of antagonist muscles during knee extension against gravity: insights for functional electrical stimulation control design*. Conf Proc IEEE Eng Med Biol Soc, 2012. **2012**: p. 1843-6.
49. Lynch, C.L. and M.R. Popovic, *A Comparison of Closed-Loop Control Algorithms for Regulating Electrically Stimulated Knee Movements in Individuals With Spinal Cord Injury*. Neural Systems and Rehabilitation Engineering, IEEE Transactions on, 2012. **20**(4): p. 539-548.
50. Qin, Z., M. Hayashibe, and C. Azevedo-Coste, *Evoked Electromyography-Based Closed-Loop Torque Control in Functional Electrical Stimulation*. Biomedical Engineering, IEEE Transactions on, 2013. **60**(8): p. 2299-2307.
51. Zhan, L., et al. *Real-time closed-loop FES control of muscle activation with evoked EMG feedback*. in *Neural Engineering (NER), 2015 7th International IEEE/EMBS Conference on*. 2015.
52. Popovic, M.R. and T.A. Thrasher, *Neuroprosthesis*. Encyclopedia of Biomaterials and Biomedical Engineering, 2004. **2**: p. 1056-1065.
53. Graham, G.M., T.A. Thrasher, and M.R. Popovic, *The effect of random modulation of functional electrical stimulation parameters on muscle fatigue*. IEEE Trans Neural Syst Rehabil Eng, 2006. **14**(1): p. 38-45.
54. Al-Amood, W.S., H.J. Finol, and D.M. Lewis, *Chronic stimulation modifies the isotonic shortening velocity of denervated rat slow-twitch muscle*. Proc R Soc Lond B Biol Sci, 1986. **228**(1250): p. 43-58.
55. Tanaka, K. and M. Sano. *Some properties of fuzzy nonlinear feedback systems*. in *Industrial Electronics, Control, Instrumentation, and Automation, 1992. Power Electronics and Motion Control., Proceedings of the 1992 International Conference on*. 1992. San Diego, CA: IEEE.
56. Tong, R.M. *Analysis of closed loop fuzzy systems*. in *Decision and Control including the Symposium on Adaptive Processes, 1979 18th IEEE Conference on*. 1979. Fort Lauderdale, FL, USA: IEEE.
57. Wang, L.-X., *Adaptive fuzzy systems and control: design and stability analysis*. 1994: Prentice-Hall, Inc. 232.
58. Ying, H., W. Siler, and J.J. Buckley, *Fuzzy control theory: A nonlinear case*. Automatica, 1990. **26**(3): p. 513-520.

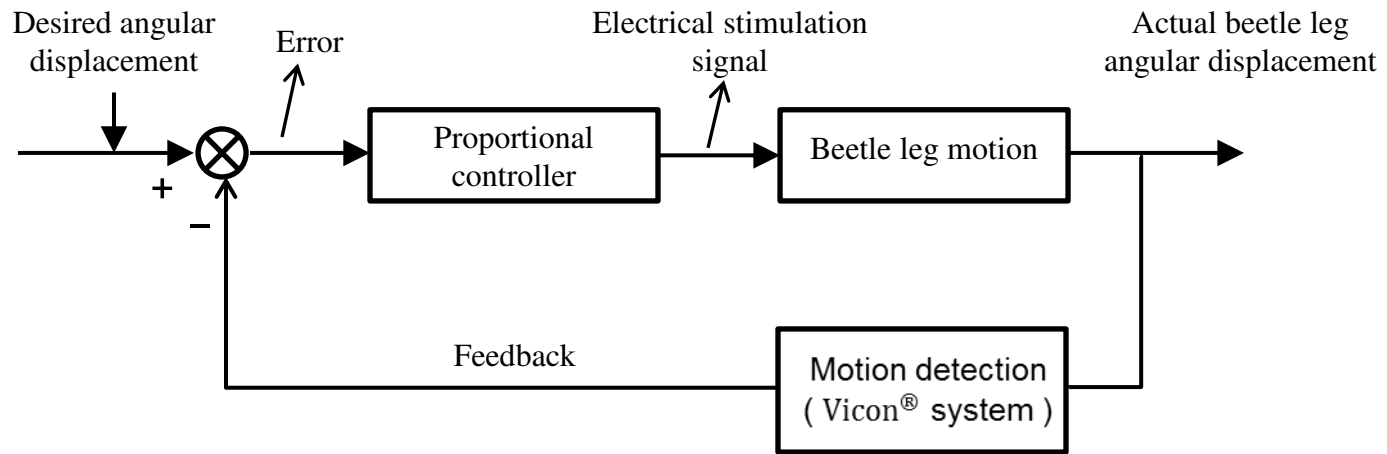
Figure





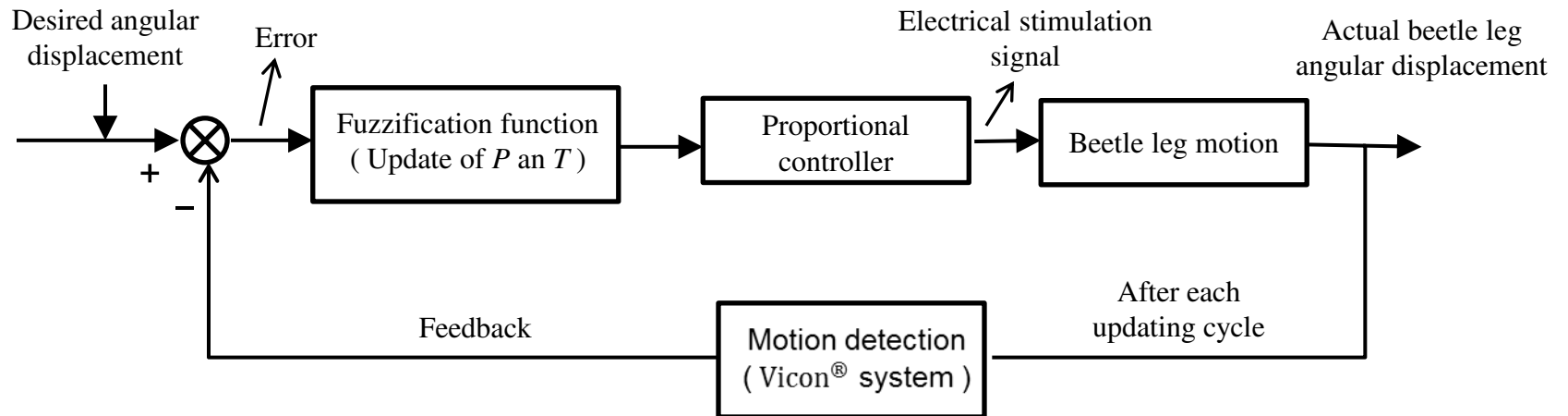
A

Conventional control system with proportional controller



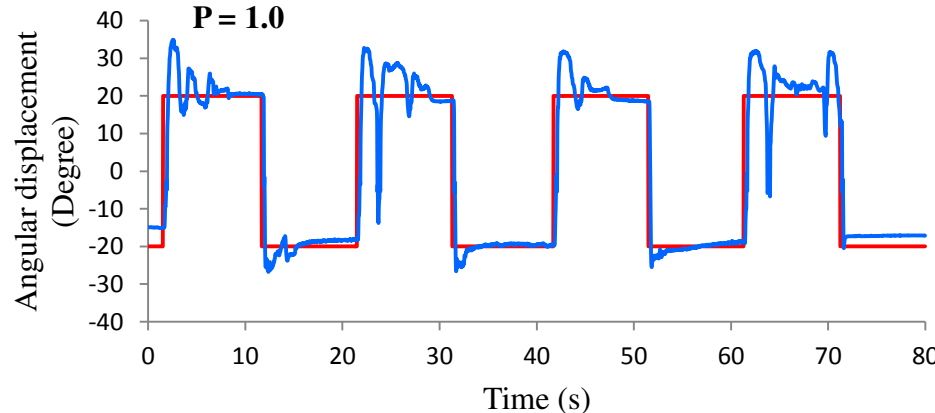
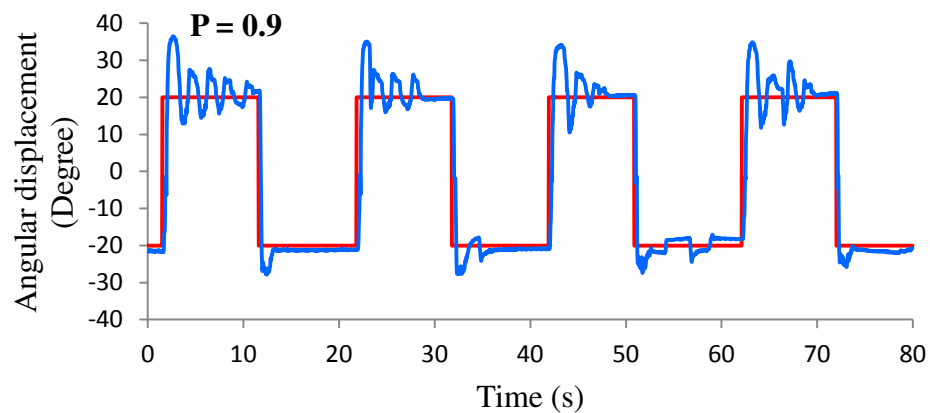
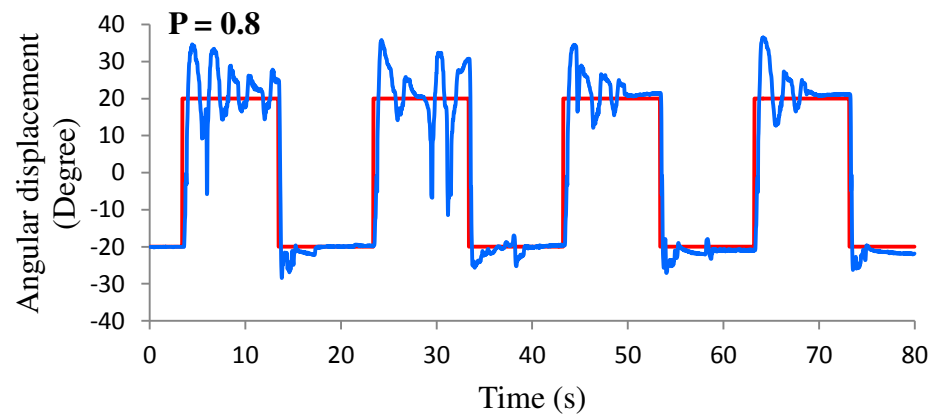
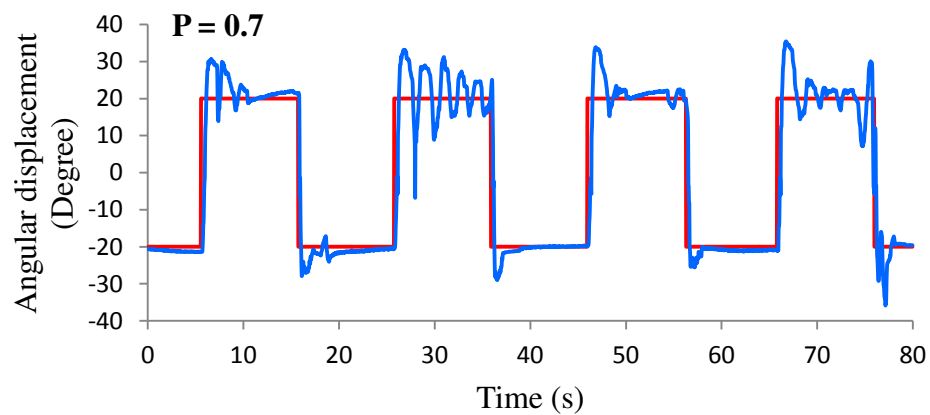
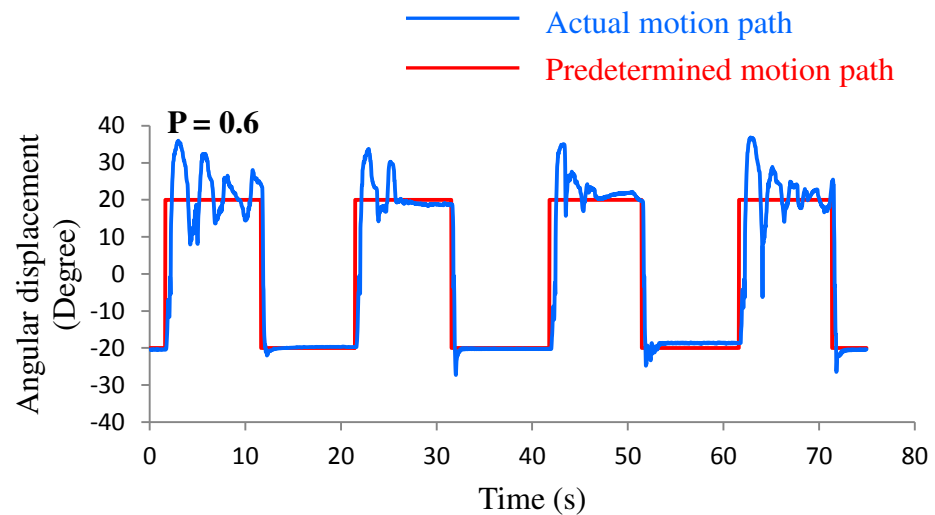
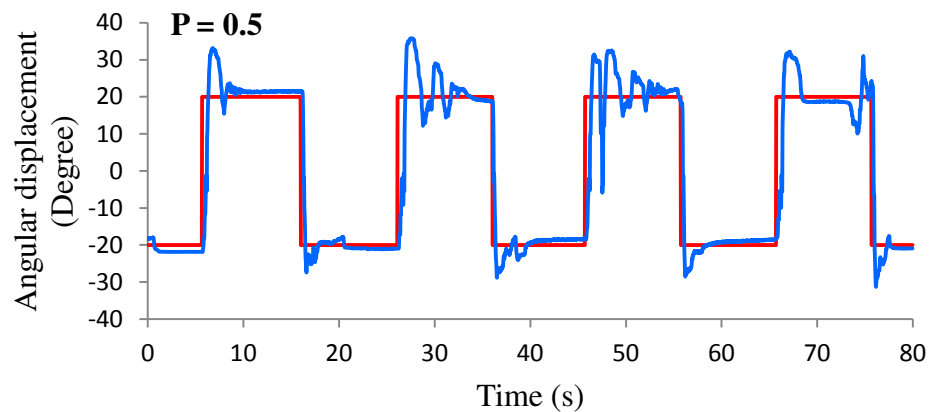
B

Fuzzy control system with multiple membership functions



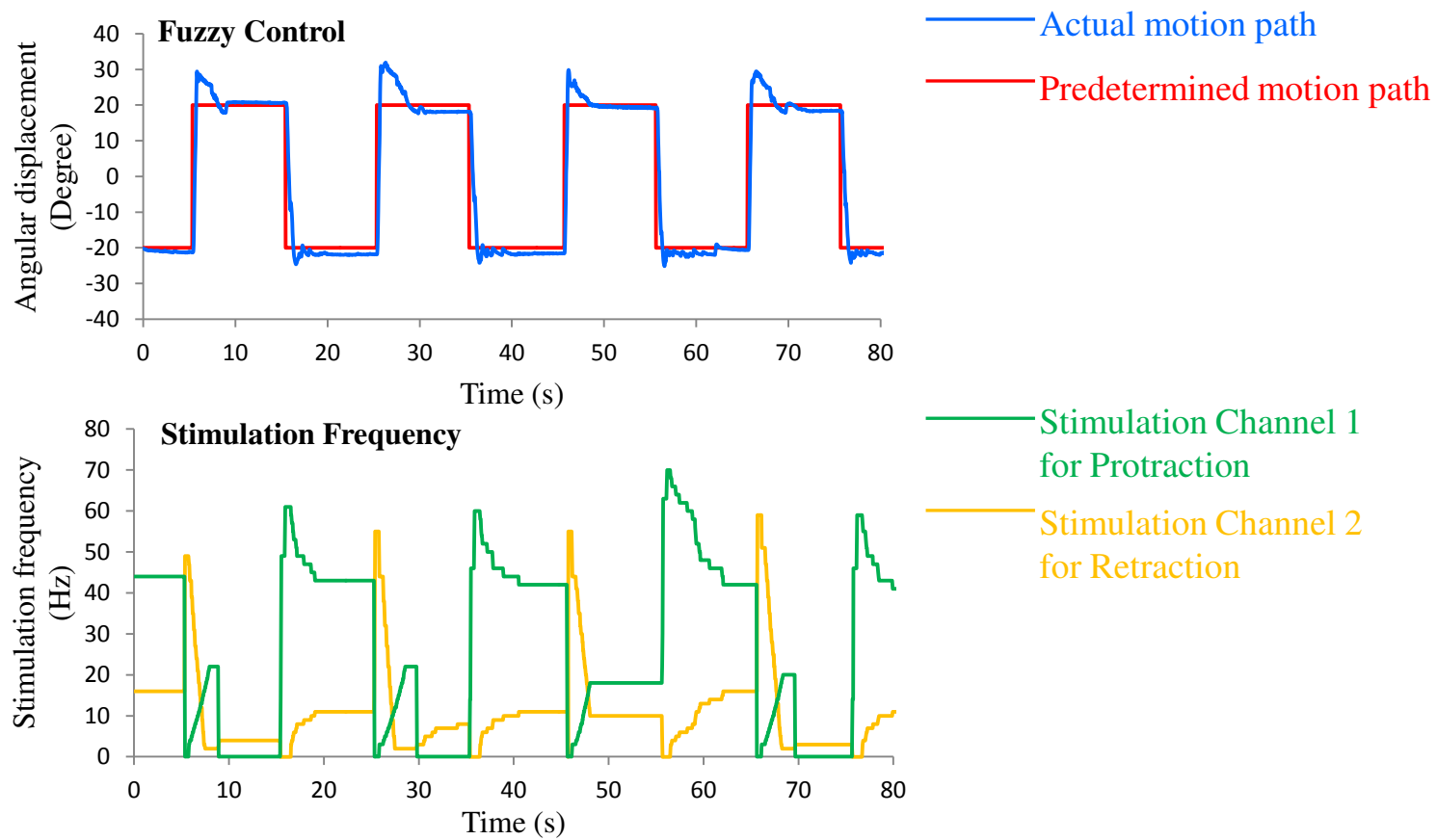
$$P/K_p = f_p(\theta_{Desired}, \theta_{Difference})$$

$$T = f_T(\theta_{Desired}, \theta_{Difference})$$

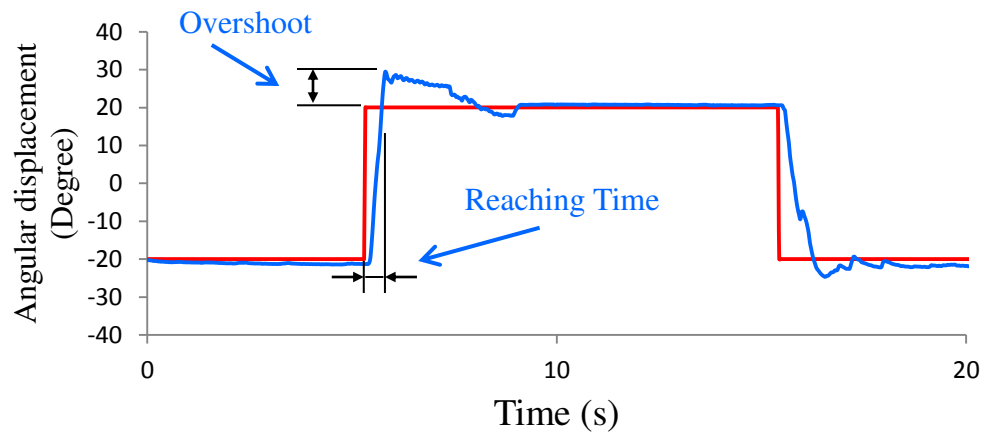


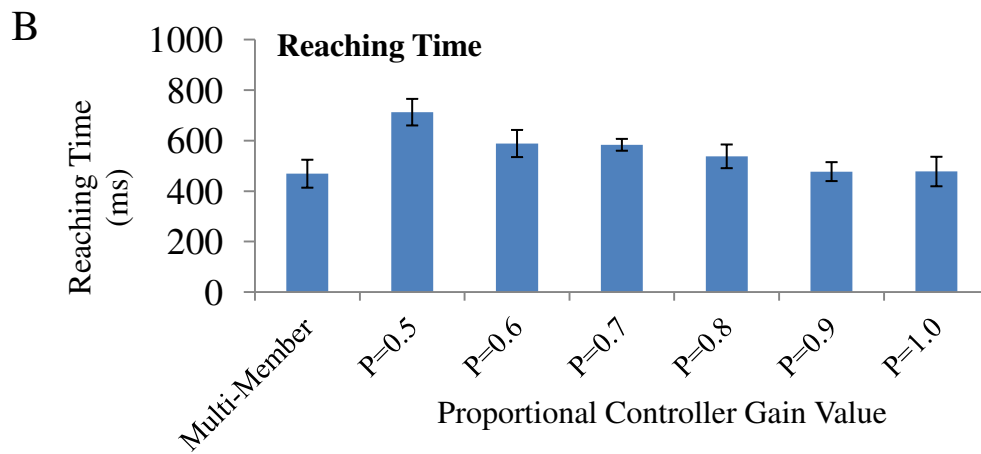
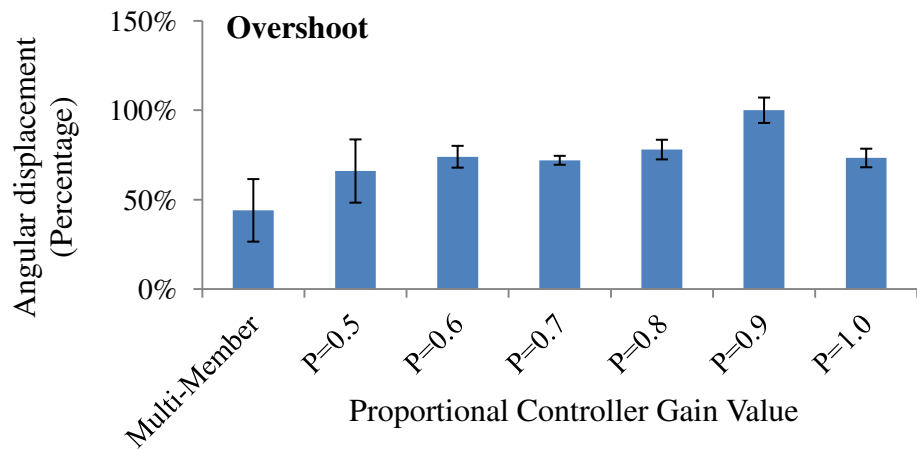
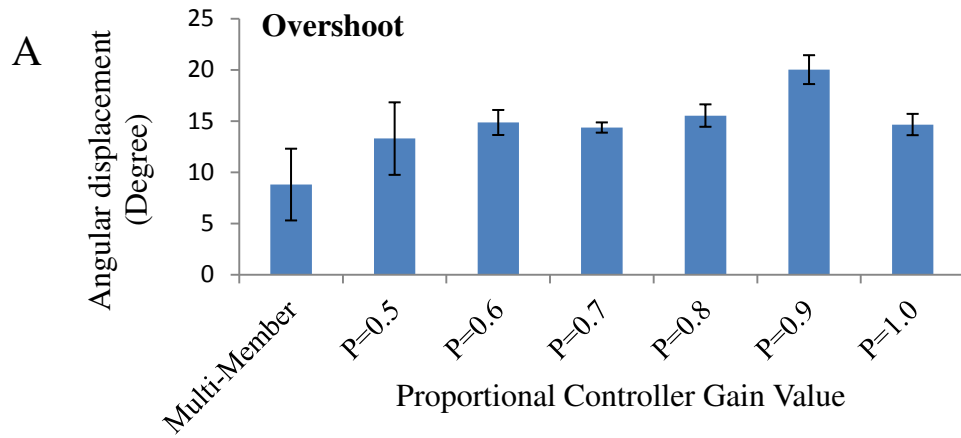
— Actual motion path
— Predetermined motion path

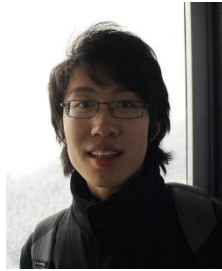
A



B



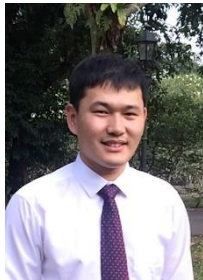




Chao Zhang graduated from Nanyang Technological University with a Bachelor in Mechanical Engineering specialized in Mechatronics, and National University of Singapore with a Master in Statistics and Applied Probability. He worked as a research assistant at Professor Sato's lab on insect-machine hybrid robot system.



Feng Cao received the B.Eng. degree in Aerospace Engineering from Nanyang Technological University, Singapore, in 2013. He joined Professor Hirotaka Sato's group to pursue his Ph.D. study at School of Mechanical and Aerospace Engineering, Nanyang Technological University in 2013. His research interest is development of both hardware and software for insect-machine hybrid robot system.



Yao Li graduated from Huazhong University of Science and Technology (China) in Jun, 2013 with a B.Eng. degree in Mechanical Engineering. Then, he joined in Dr. Sato's group at Nanyang Technological University (Singapore) as a Ph.D. student in Aug, 2013. The interests of this group cover a range of topics in insect-machine hybrid system. Currently his research topics are mainly in the insect flight control and insect body attitude analysis.



Hirotaka Sato is currently an assistant professor working on insect-machine hybrid robots at School of Mechanical & Aerospace Engineering, Nanyang Technological University, Singapore. He previously worked on that research at Department of Electrical Engineering and Computer Science at University of California at Berkeley (2008 – 2011) and University of Michigan (2007). He received Ph.D.(2005), Master (2002) and B.S degrees (2000) from Waseda University for his nano/micro fabrication processes for MEMS.